The Journal of Experimental Biology 208, 2333-2346
Published by The Company of Biologists 2005
doi:10.1242/jeb.01661

Effect of an increase in gravity on the power output and the rebound of the body in human running

G. A. Cavagna[1,*], N. C. Heglund[2] and P. A. Willems[2]

[1]*Istituto di Fisiologia Umana, Università degli Studi di Milano, 20133 Milan, Italy* and [2]*Unité de Physiologie et Biomécanique de la Locomotion, Université catholique de Louvain, 1348 Louvain-la-Neuve, Belgium*

*Author for correspondence (e-mail: giovanni.cavagna@unimi.it)

Accepted 25 April 2005

Summary

The effect of an increase in gravity on the mechanics of running has been studied by using a force platform fixed to the floor of an aircraft undergoing flight profiles, resulting in a simulated gravity of 1.3 *g*. The power spent to maintain the motion of the centre of mass of the body is ~1.3 times greater than on Earth, due to a similar increase of both the power spent against gravity and to sustain the forward speed changes. This indicates that the average vertical displacement per unit distance and the average direction of the push are unchanged. The increase in power is mainly due to an increase in step frequency rather than to an increase in the work done at each step. The increase in step frequency in turn is mainly due to a decreased duration of the effective aerial phase (when the vertical force is less than body weight), rather than an increase in the stiffness of the bouncing system. The maximal speed where step frequency can match the resonant frequency of the bouncing system is increased by ~5 km h^{-1} at 1.3 *g*. These results suggest a similar running mechanics at higher gravity, maintained at the expense of greater energy expenditure.

Key words: locomotion, running, gravity, human.

Introduction

In both walking and running the body decelerates forwards at each step. The braking action is due to the more-or-less extensible link represented by the supporting anatomical structures interposed between the centre of mass of the body and the point of contact on the ground. In order to maintain the average speed constant, it is necessary to reaccelerate the centre of mass forwards each step, and this occurs when the point of contact of the foot on the ground is behind the centre of mass. Chemical energy is spent to maintain the muscles active during both the brake (negative work) and the subsequent forward acceleration (positive work). It follows that the fluctuations in kinetic energy of forward motion imply a waste of energy.

The waste of energy during legged terrestrial locomotion is reduced by two basic mechanisms: the pendular mechanism of walking and the bouncing mechanism of running. In walking, the kinetic energy of forward motion is stored in part as gravitational potential energy when the point of contact with the ground is in front of the centre of mass: the body is lifted while it decelerates forwards. The process is reversed when the point of contact is behind the centre of mass with a transformation of potential energy back into kinetic energy of forward motion. Gravitational potential energy and kinetic energy of forward motion change in opposition of phase during a walking step (Cavagna et al., 1963).

The same energy conserving mechanism is not possible in running because the centre of mass is lowered while decelerating forwards and lifted while accelerating forwards. Gravitational potential energy and kinetic energy of forward motion change in-phase during the running step (Cavagna et al., 1964). With each step the muscle–tendon units must absorb and restore both the kinetic energy change of forward motion, due to the braking action of the ground, and the gravitational potential energy change, associated with the fall and the lift of the centre of mass. This results in a large amount of negative and positive work and the chemical energy cost per unit distance is twice that spent in walking at the optimal speed (Margaria, 1938).

The metabolic energy expenditure is reduced in running, however, by an elastic storage and recovery of mechanical energy, as in a bouncing ball. This was initially suggested by the finding that in human running the ratio between mechanical power output and metabolic energy expenditure exceeded the maximum efficiency of transformation of chemical energy into mechanical work (Cavagna et al., 1964). Evidence for an elastic storage and recovery was also found in the kangaroo by Alexander and Vernon (1975) and in the horse by Biewener (1998). A spring–mass model of the bounce of the body at each running step (Blickhan, 1989; McMahon and Cheng, 1990; Seyfarth et al., 2002) is now widely used in studies on the effect of the spring stiffness on energy expenditure (McMahon et al., 1987; Kerdok et al., 2002) as well as the changes in

spring stiffness and step frequency with speed (Cavagna et al., 1988; McMahon and Cheng, 1990) and with surfaces of different stiffness (Ferris and Farley, 1997; Ferris et al., 1998; 1999; Kerdok et al., 2002).

As expected, the pendular mechanism of walking is drastically affected by gravity. The range of walking speeds, optimal walking speed and external work done to move the centre of mass are all increased by gravity (Cavagna et al., 2000). Walking on the Moon is practically not possible (Margaria and Cavagna, 1964): in fact, locomotion takes place by a succession of bounces with a mechanism similar to that of running on Earth. The effect of gravity on the mechanism of running still needs investigation. Suspending the body from springs results in a reduction of the peak force attained at each step during running, with little change of the stiffness of the leg (He et al., 1991). No data exist on the effect of an increase in gravity on the mechanics of running.

One purpose of the present study was to analyze the effect of an increase in gravity on the characteristics of the elastic bounce of the body. The vertical oscillation of the centre of mass during each running step can be divided into two parts: one taking place when the vertical force exerted on the ground is greater than body weight (lower part of the oscillation) and another when this force is smaller than body weight (upper part of the oscillation; Fig. 1). According to the spring–mass model, the duration of the lower part of the oscillation represents half-period of the bouncing system and the vertical displacement of the centre of mass during this period represents the amplitude of the oscillation (Cavagna et al., 1988; Blickhan, 1989; McMahon and Cheng, 1990). The upper part of the oscillation, by contrast, may be compared with the second half-period only in the absence of an aerial phase, as often happens during trotting and very slow running (Cavagna et al., 1988) (Fig. 1). On Earth, the rebound is symmetric, i.e. the duration and the amplitude of the lower part of the oscillation are about equal to those of the upper part up to a speed of ~11 km h^{-1} in both adult humans and children (Cavagna et al., 1988; Schepens et al., 1998). It follows that up to this critical speed the step frequency equals the frequency of the bouncing system. Above the critical speed the rebound becomes asymmetric, i.e. the duration and the amplitude of the upper part of the oscillation become greater than those of the lower part, and the step frequency is lower than the frequency of the system. The asymmetry arises because the average vertical acceleration upwards during the lower part of the oscillation becomes greater than 1 ***g***, whereas during the upper part of the oscillation the average vertical acceleration downwards cannot exceed 1 ***g***. It was therefore suggested that the critical speed may depend on gravity and that at higher gravity values this speed would probably be greater (Schepens et al., 1998). The aim of the present study was therefore to determine experimentally if and to what extent this hypothesis is true. Analysis of the rebound of the body may also help to determine how an increase in gravity affects the stiffness of the bouncing system and the preferred combination between stiffness and landing angle of attack (Seyfarth et al., 2002).

A second question was the effect of an increase in gravity on the external mechanical work done to sustain the displacements of the centre of mass of the body in the sagittal plane. In walking, external work increases with gravity in both its components: the work against gravity and the work to sustain the forward velocity changes, the former increasing much more than the second. It is likely that gravity will also increase the external work in running, but the amount of this increase is not known, nor to what extent it will affect the work done against gravity and the work done to sustain the forward velocity changes.

In order to answer the questions outlined above, the motion of the centre of mass of the body during running at different speeds was analyzed in this study on Earth and on an aeroplane undergoing flight profiles, resulting in a simulated gravity of 1.3 ***g***. The effect of the increase in gravity on the stiffness of the bouncing system and on the work done to move the centre of mass in a sagittal plane was measured.

Materials and methods

The experimental procedure consisted of measuring the vertical and fore–aft components of the force exerted by feet on a large force platform. The parameters characterizing the bounce of the body, such as the whole body vertical stiffness, leg stiffness, vertical and horizontal displacements of the centre of mass of the body during contact and during the effective time of contact, were measured as described by Cavagna et al. (1988) and McMahon and Cheng (1990). The mechanical energy changes of the centre of mass of the subject during one or more subsequent running steps were determined from the force platform records as described by Cavagna (1975). Details of the subjects, the hardware and the software used are given below.

Subjects

The experiments were made on five adult subjects, four males: A, 33 years, 68–72 kg, 1.74 m height, leg length (hip to floor) 0.92 m; B, 68 years, 81 kg, 1.79 m height, leg length 0.94 m; C, 53 years, 87–91 kg, 1.93 m height, leg length 1.03 m; D, 46 years, 87 kg, 1.79 m height, leg length 0.93 m; and one female E, 25 years, 52 kg, 1.66 m height, leg length 0.87 m. Informed consent was obtained from each subject. The studies were performed according to the Declaration of Helsinki. The European Space Agency Safety Committee approved the procedures in the experiments made on the aeroplane.

Experiments at 1.3 **g**

Experiments were performed during the 32nd European Space Agency parabolic flight campaign. A simulated gravity of 1.3 ***g*** was attained during turns of an A300 Airbus. The experiments were done over 3 days with a total of 23 turns. An aircraft orthogonal frame of reference was defined as follows: the *X*-axis is parallel to the fore–aft axis of the aeroplane, the *Y*-axis is parallel to the lateral axis of the aeroplane and the *Z*-axis is perpendicular to the floor of the aeroplane. Three accelerometers (DS Europe, Milan, Italy) measured simultaneously the *X*, *Y* and *Z* components of the acceleration

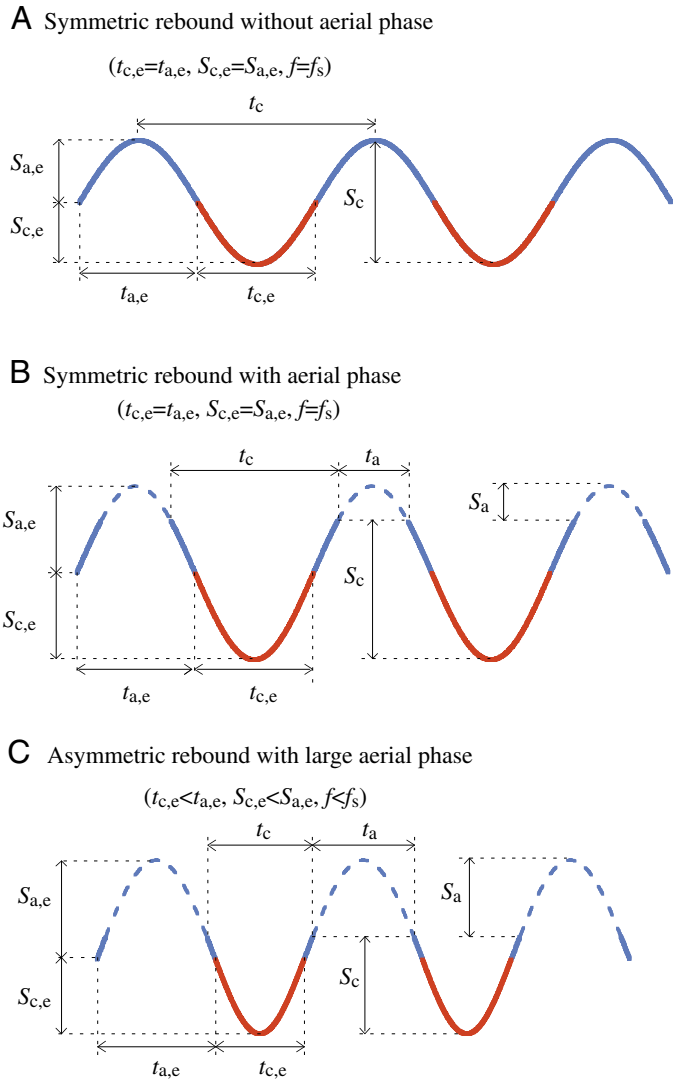

Fig. 1. Diagrammatic representation of the effective aerial and contact times, and vertical displacements. The vertical displacement of the centre of mass during the time of contact with the ground t_c (continuous line) and during the aerial phase t_a (broken line) is divided into a lower part S_{ce} (red) taking place when the vertical force is greater than body weight, and into an upper part S_{ae} (blue) taking place when the vertical force is less than body weight. Running speed increases from top to bottom. Note that in all cases S_{ce} (red) represents the amplitude of the oscillation of the spring–mass system from its equilibrium point and its duration t_{ce} represents a half period of the oscillation (neither the peak-to-peak vertical displacement nor the vertical displacement during contact represent the amplitude of the oscillation). S_{ae} (blue) represents the amplitude of the oscillation in the opposite direction, and its duration t_{ae} the half period of the oscillation, only at the lowest running speed (A) when the whole vertical displacement takes place during contact S_c. Only A, when no aerial phase takes place, is consistent with the spring–mass model. With increasing speed a progressively greater fraction of the vertical displacement takes place during the aerial phase S_a. The resonant frequency of the spring–mass system $f_s=1/(2t_{ce})$ equals the step frequency f only when $t_{ce}=t_{ae}$, i.e. when the rebound is symmetric (A,B). At high running speeds (C) the rebound is asymmetric ($t_{ce}<t_{ae}$) and the step frequency is lower than the resonant frequency of the system.

vector in the aircraft reference frame. In order to reduce the noise induced by the aircraft vibrations (Fig. 2), the accelerometers were both mechanically and electrically damped by a low-pass filter with a cut-off frequency at 5 Hz. In this study, results are given as means ± S.D. During the time intervals encompassing the 175 steps analysed, the acceleration was 12.90±0.51 m s^{-2} in the Z-direction, 0.03±0.06 m s^{-2} in the X-direction and 0.13±0.16 m s^{-2} in the Y-direction. The X and Y-axis accelerations of the frame of reference were neglected and the acceleration along the Z-axis of the frame of reference was considered to be equivalent to the vertical on Earth. Therefore in the following text, forward (or fore–aft), lateral, and vertical refer to the X, Y and Z-axes, respectively.

During each turn, the subjects ran at different speeds back and forth across a 6.1 m×0.4 m force platform fixed to the aeroplane floor along the X-axis. The platform (Heglund, 1981) was sensitive to the force exerted by the feet in the forward (X) and vertical (Z) directions; lateral (Y) forces were neglected. The lowest frequency mode of vibration for the unloaded platform was greater than 180 Hz. With each turn of the aircraft, the simulated gravity was maintained for 40–60 s: during this period the subjects could run several times back and forth on the platform, one after the other. Two handrails, fixed on each side of the platform, proved to be useful in case the subject lost balance. Two photocells fixed 5.87 m apart at neck height along the side of the platform were used to determine the average running speed, $\overline{V}_f$. Two additional photocells, 1.93 m from the first and last, were used to detect rough variations in speed between the first and the last photocells. Two video cameras were used to check for obvious loss in balance or touching the handrails. Before stepping on the platform, the subjects had, in one direction, 12 m to accelerate, the last 6 m of which were at the same level of the platform; the corresponding figures in the other direction were 8 and 4.8 m.

Data were gathered as follows. The five subjects made 309 runs, of which 175 were used for analysis. The other runs were unusable because the subject was accelerating or decelerating forward (indicated by a continuous velocity change greater than 0.3 m s^{-1} from start to end of the run), lost balance, made irregular steps, the platform signals were out of scale, records between photocells were incomplete or the Z, Y and X acceleration were not steady due to turbulence or other factor. In particular, of the 175 runs analysed: subject A had 50 runs with 61 steps analysed (speed range: 5.8–20.5 km h^{-1}); B had 20 runs with 31 steps analysed (6.0–13.6 km h^{-1}); C had 12 runs with 16 steps analysed (7.5–11.2 km h^{-1}), D had 47 runs with 61 steps analysed (5.5–15.5 km h^{-1}); and E had 46 runs with 52 steps analysed (5.2–15.3 km h^{-1}).

A microcomputer was used at a sampling rate of 500 Hz to acquire (i) the platform signals, proportional to the force exerted by the feet in forward direction (F_f, along the X-axis of the aeroplane) and in vertical direction (F_v, along the Z-axis of the aeroplane), (ii) the output of photocell circuit, and (iii) the output of the accelerometers (Fig. 2). No subject suffered motion sickness. Subjects experienced a normal coordination of movements since the first runs at 1.3 $\boldsymbol{g}$, but at an evidently

greater effort; any instability tended to quickly result in a loss of balance due to the greater vertical acceleration.

Experiments at 1 **g**

Data were gathered during running in the laboratory of Louvain-la-Neuve with the same platform used on the aeroplane (photocell distance 3–4.5 m according to the running speed) and in the laboratory of Milan with the platform described by Cavagna (1975; photocells distance 3 m). The two platforms gave consistent results. Data were collected for the same range of speeds obtained by each subject on the aeroplane (5–20 km h^{-1}). Subject A had 32 runs with 45 steps analysed (made before the flight, sampling frequency 500 Hz); B had 20 runs with 23 steps analysed (three before the flight, 250–500 Hz, the others after the flight, 500 Hz); C had 14 runs with 25 steps analysed (after the flight, 500 Hz), E had 25 runs with 36 steps analysed (after the flight, 200–400 Hz); D had 29 runs with 47 steps analysed (23 before the flight and 6 after, 500 Hz). Experimental records obtained at 1 ***g*** and at 1.3 ***g*** are given in Fig. 2.

Analysis of force platform records

A custom LabVIEW (6.1) software program was used to analyze the ground reaction force records. The average of the first 50 points of the unloaded platform base lines was measured in the short time interval between runs and subtracted from the entire F_f and F_v arrays to get the net changes of F_f and F_v during each run. In case of the 1.3 ***g*** experiments, the F_f and F_v records where also corrected at each instant for the changes in acceleration during the aircraft manoeuvres. This was made by subtracting the product of the changes in the acceleration measured by

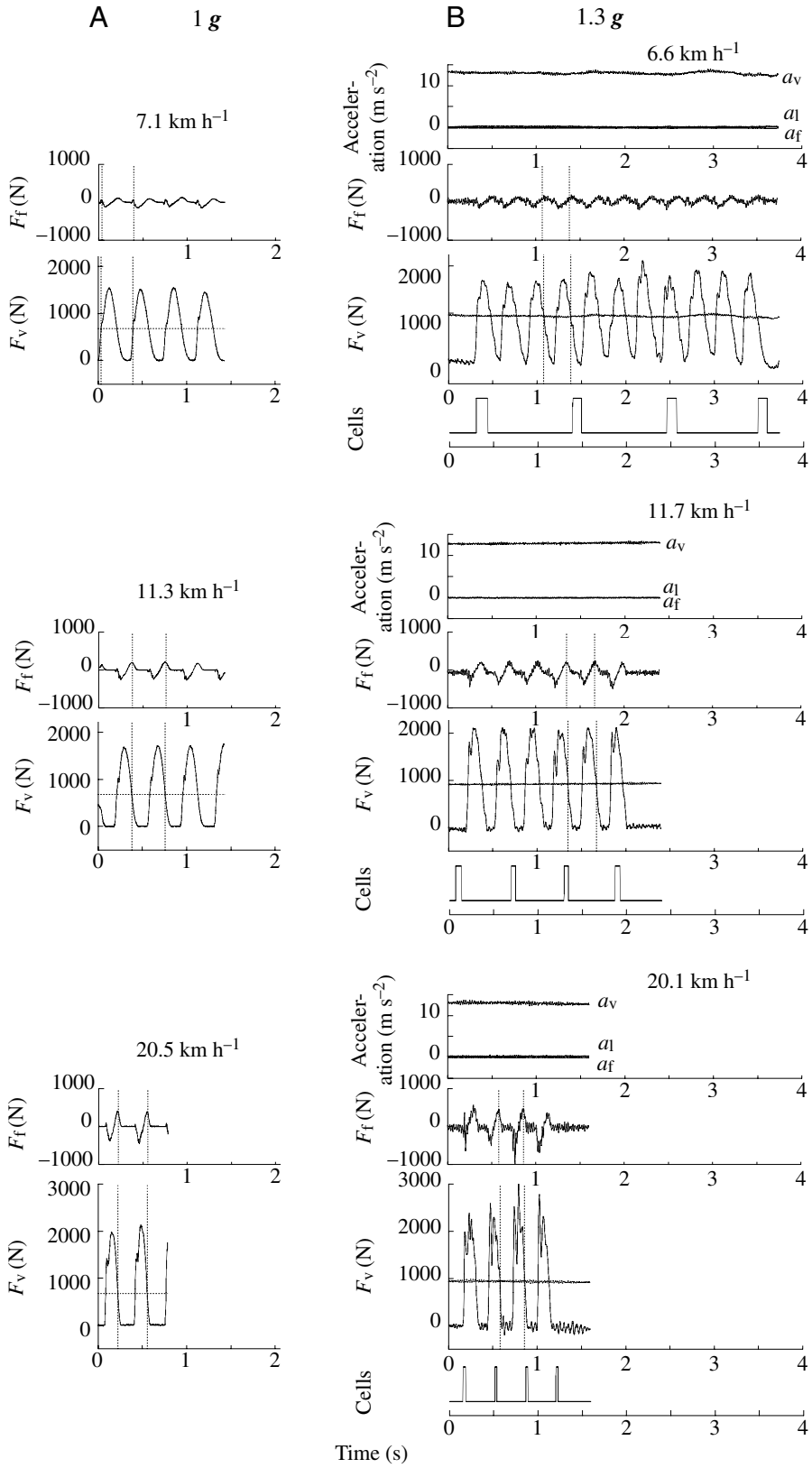

Fig. 2. Experimental records of running on Earth (A) and during a flight profile simulating 1.3 ***g*** (B). (A) Fore–aft (F_f) and vertical (F_v) components of the force exerted by the foot on the force platform during running between the two photocells at the indicated speeds on Earth. (B) From top to bottom at each speed are shown the vertical (a_v), lateral (a_l), and fore–aft (a_f) components of the acceleration recorded on the aircraft during the run; the force signals F_f and F_v from the force platform (noise is due to vibrations of the aircraft) and the output of the photocell circuit. The vertical dotted lines delimit the time interval corresponding to the steps illustrated in Fig. 3, with expansion of the energy records to include the previous valley of potential energy as described in the Materials and methods. Subject A, mass 72 kg.

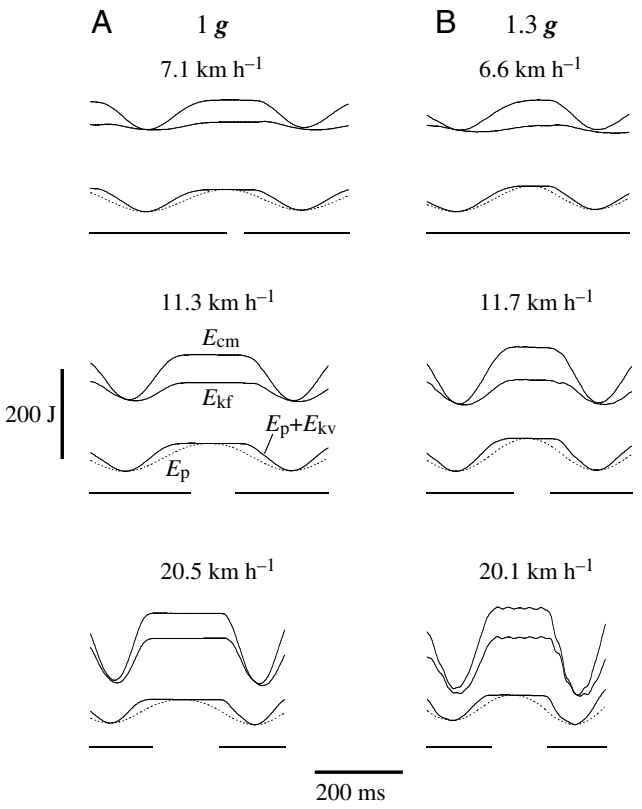

Fig. 3. Mechanical energy changes of the centre of mass of the body during the running step. (A) 1 ***g***, (B) 1.3 ***g***. At each speed the curves show from bottom to top: the changes in the gravitational potential energy of the centre of mass of the body (E_p, dotted line), the sum of the kinetic energy of vertical motion (E_{kv}) plus E_p (continuous line), the kinetic energy of forward motion (E_{kf}) and the total translational energy of the centre of mass in the sagittal plane ($E_{cm}=E_p+E_{kv}+E_{kf}$). The records were obtained as described in the Materials and methods from the F_v and F_f signals for the steps indicated by the vertical interrupted lines in Fig. 2, expanded to the left to include the previous valley of E_p. At each speed, the zero line corresponds to the minimum attained by the E_p curve. The continuous line below each panel indicates the ground contact time.

the accelerometers along the *Z* and *X*-axis times the mass of the suspended part of the platform.

An integer number of running steps, encompassing those subsequently used for calculation, was selected between peaks of F_v. The time-average of the F_v record over an integer number of cycles should equal body weight. In reality the ratio between this time-average and the weight of the subject (body mass × 1.0 ***g*** for the Earth experiments and ≈1.3 ***g*** for the aeroplane experiments) was 1.00±0.02 (N=120) in the experiments at 1 ***g*** and 1.05±0.05 (N=175) at 1.3 ***g***.

The velocity of the centre of mass of the body in the vertical direction V_v and in the forward direction V_f was determined by integration of the F_v and F_f tracings (Cavagna, 1975). Only translational motion in a sagittal plane was considered when calculating the mechanical energy of the centre of mass. Lateral movements were ignored.

The instantaneous vertical velocity $V_v(t)$ was used to calculate the instantaneous kinetic energy of vertical motion $E_{kv}(t)=0.5M_bV_v(t)^2$ and, by integration, the vertical displacement of the centre of mass, $S_v(t)$, with the corresponding gravitational potential energy change $E_p(t)=M_b\boldsymbol{g}S_v(t)$. The kinetic energy of forward motion was calculated as $E_{kf}(t)=0.5M_bV_f(t)^{2,}$ the total translational kinetic energy of the centre of mass in the sagittal plane as $E_k(t)=E_{kf}(t)+E_{kv}(t)$, and the translational mechanical energy of the centre of mass in the sagittal plane as $E_{cm}(t)=E_{kv}(t)+E_{kf}(t)+E_p(t)$ (Fig. 3).

Since this study refers to steady running at a constant step-average speed, an integer number of running cycles was selected between two V_v peaks (or valleys), searching by eye for a minimum difference between the beginning and the end of both the V_v and V_f records. The time-average vertical velocity in the selected integral number of V_v cycles was calculated and considered to be zero on the assumption that the upward vertical displacement was equal to the downward vertical displacement (Cavagna, 1975). This would only be true if successive steps were exactly equal to each other. An attempt to quantify the consequences of this assumption is described below.

The work done at each step to move the centre of mass in the sagittal plane was measured in the interval included between two or more peaks (or valleys) of the gravitational potential energy, E_p. Since, as mentioned above, selection was initially made between peaks (or valleys) of the vertical velocity, the record was expanded to include the previous valley (or peak) of $E_p(t)$ until a clear picture of the selected steps was obtained (Fig. 3). The work done during the selected steps, W_v, W_k, W_{kf} and W_{ext}, was calculated from the amplitudes of peaks and valleys and the initial and final values in the $E_p(t)$, $E_k(t)$, $E_{kf}(t)$ and $E_{cm}(t)$ records. Positive values of the energy changes gave positive work, negative values gave negative work. In a perfectly steady run on the level the ratio between positive and negative work should be equal to one. In reality the ratios were as follows. In the 1 ***g*** experiments (N=120): W^+_v/W^-_v=1.00±0.04, W^+_k/W^-_k= 1.01±0.06, W^+_{kf}/W^-_{kf}=1.02±0.10, W^+_{ext}/W^-_{ext}= 1.01±0.05. In the 1.3 ***g*** experiments (N=175): W^+_v/W^-_v=1.01±0.10, W^+_k/W^-_k= 1.01±0.10, W^+_{kf}/W^-_{kf}=1.02±0.16, W^+_{ext}/W^-_{ext}=1.01±0.09.

The error involved by the assumption that lifts equal falls in an integer number of steps was estimated from the difference in amplitude between the first and last of the selected $V_v(t)$ peaks (or valleys), as if this difference were due to a drift of the whole $V_v(t)$ record. Accordingly, the absolute value of the difference between $V_v(t)$ peaks (or valleys) was multiplied by the time interval between them and divided by 2 to get the vertical displacement due to the hypothetical drift. This was then expressed as a fraction of the sum of the upward vertical displacements calculated during the same time interval: 0.08±0.07 at 1 ***g*** (N=120) and 0.15±0.12 at 1.3 ***g*** (N=175). These figures correspond to a random error less than 1% in the measured values of E_p (as found by simulating the V_v drift over one step with a sine wave).

Aerial time and vertical displacement during contact

Since the mechanical energy of the centre of mass is constant when the body is airborne (air resistance is neglected),

the aerial time was calculated as the time interval during which the derivative $dE_{cm}(t)/dt=0$. This time interval was measured using two reference levels set by the user above and below the section of the record where $dE_{cm}(t)/dt\approx0$. When vibrations or a peak of E_{cm} at the end of the aerial phase (at high speeds) disturbed this measurement, the aerial time could also be determined by eye on the basis of the duration of the plateau of the $E_{cm}(t)$ record (Fig. 3, after appropriate expansion of the tracing): this procedure, however, was followed in only eight of the 295 runs analyzed. The upward and downward displacement of the centre of mass during contact was measured from the section of the $E_p(t)$ curve during which $dE_{cm}(t)/dt\neq0$ and $dE_p(t)/dt$ was positive and negative, respectively.

'Effective' contact and aerial times, vertical and forward displacements

As described in the Introduction, the spring–mass model can be applied to the vertical displacement of the centre of mass taking place at each running step provided that the period and the amplitude of the oscillation of the spring–mass system are correctly measured. In all conditions the half period of the oscillation equals the time interval where the centre of mass decelerates downwards and accelerates upwards, i.e. the time interval during which the vertical force is greater than body weight. This time interval is called effective contact time, t_{ce}, and is shorter than the total time of contact (Fig. 1). The time interval where the centre of mass decelerates upwards and accelerates downwards, i.e. when the vertical force is less than body weight, is called effective aerial time, t_{ae}: it occurs both during contact and during the aerial phase and does not necessarily correspond to the other half period of the oscillation. The amplitude of the vertical oscillation, i.e. the compression of the spring from its equilibrium position, equals in all conditions the vertical displacement S_{ce} attained during t_{ce}. The displacement upward, S_{ae}, attained during t_{ae} corresponds to the amplitude of the vertical oscillation only in the

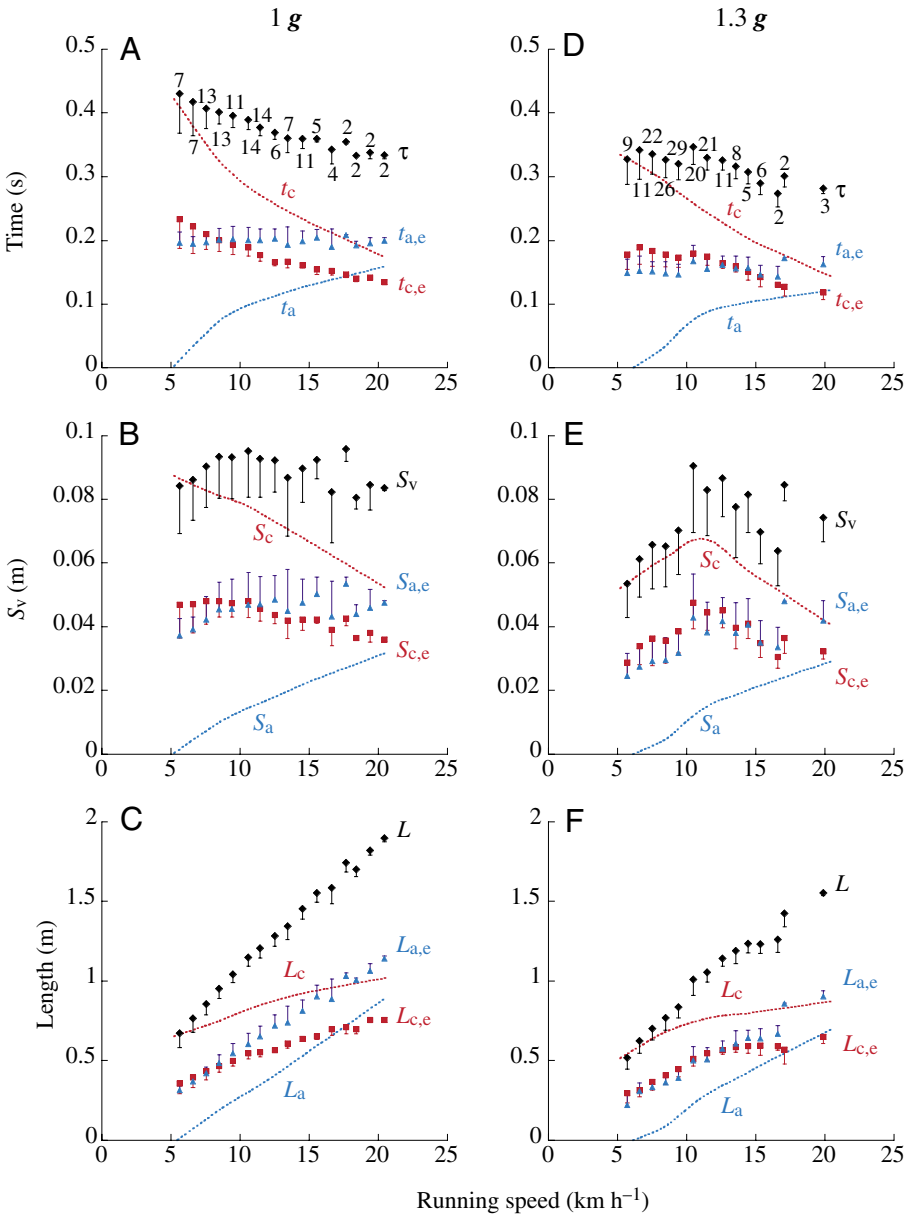

Fig. 4. Step duration and displacements of the centre of mass in vertical and forward direction as a function of running speed. (A–C) 1 ***g***, (D–F) 1.3 ***g***. Diamonds (black) indicate, from top to bottom, the step period (τ), the vertical displacement of the centre of gravity of the body during the step (S_v) and the step length (L) as a function of the running speed ($\overline{V}_f$). Triangles (blue) indicate the duration (t_{ae}) of the effective aerial phase, and the displacement of the centre of gravity during this phase in the vertical direction (S_{ae}) and in the forward direction (L_{ae}). Similarly, squares (red) indicate the duration (t_{ce}) of the effective contact phase and the corresponding displacements in the vertical direction (S_{ce}) and in the forward direction (L_{ce}). The red broken line in each panel indicates the actual contact time (t_c), and the vertical (S_c) and forward (L_c) displacement of the centre of mass during it. The blue broken line in each panel indicates the actual aerial time (t_a), and the vertical (S_a) and forward (L_a) displacement of the centre of mass during it. The vertical bars indicate the standard deviation of the mean calculated in each velocity class; the figures near the symbols in the upper panels indicate the number of items in the mean. Note that the step divisions based on the effective contact time and aerial time correspond to about half of total duration and displacements of the step, whereas the fraction of the step occupied by the actual contact and aerial phases varies widely with speed. Note also that the speed beyond which $t_{ae}=t_{ce}$, $S_{ae}=S_{ce}$ and $L_{ae}=L_{ce}$ is greater at 1.3 ***g*** than at 1 ***g***.

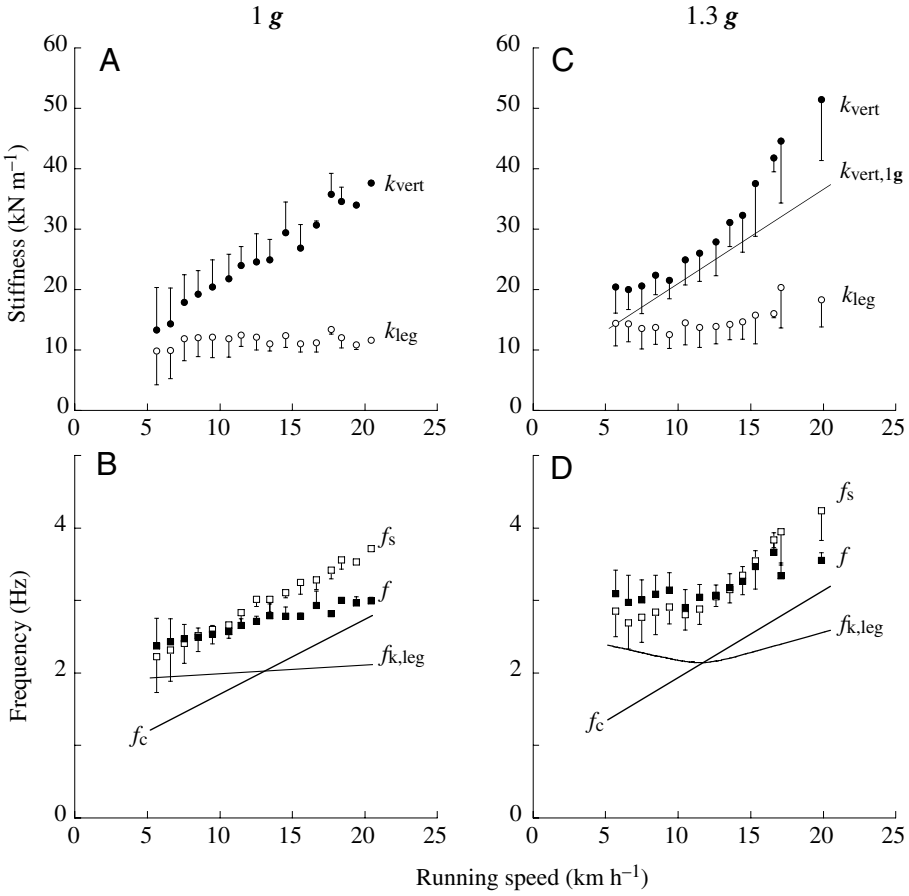

Fig. 5. Stiffness (A,C), resonant frequency of the bouncing system and freely chosen step frequency (B,D) as a function of running speed. (A,B) 1 ***g***, (C,D) 1.3 ***g***. In A and C, filled circles give the vertical stiffness of the bouncing system [$k_{vert}=M_b(\pi/t_{ce})^2$], whereas open circles give the leg stiffness (k_{leg}), calculated as described in the Materials and methods. The $k_{vert,1g}$ line in C is drawn for comparison to show the similarity of the two stiffness at intermediate speeds. In B and D, filled squares indicate the freely chosen step frequency (f) for comparison with open squares, the resonant frequency of the bouncing system [$f_s=1/(2t_{ce})$], calculated assuming that the effective contact time corresponds to one half-period of the oscillation of the elastic system. Note that the increase in gravity increases the maximum speed where $f=f_s$. The two lower lines indicate the frequency $f_{k,leg}=(k_{leg}/M_b)^{0.5}/(2\pi)$, calculated from the leg stiffness and the frequency $f_c=1/(2t_c)$, calculated assuming that the time of contact corresponds to one half-period of the oscillation of the elastic system: both give false indication in their relation with the actual step frequency. Lines are least-squares linear regressions or weighted mean of all the data (Kaleidagraph 3.6.4).

absence of an aerial phase (Cavagna et al, 1988). In the spring–mass model, but not in the actual running step (see below), both S_{ce} and S_{ae} are assumed to be equal during the lift and the fall of the centre of mass.

The locations of the E_{kv} peaks attained during the step were used in this study to determine the transition from the effective aerial time to the effective contact time and *vice versa*. The locations and the amplitudes of E_p simultaneous with the peaks of E_{kv} were used to determine the vertical displacements, $S_{ce,down}$, during the downward deceleration of the centre of mass, and $S_{ce,up}$, during the upward acceleration of the centre of mass. Since $S_{ce,down}$ may differ from $S_{ce,up}$, the amplitude of the oscillation was taken as $S_{ce}=(S_{ce,down}+S_{ce,up})/2$ (Fig. 4). The downward and upward vertical displacements during the effective aerial phase were calculated as $S_{ae,down}=S_{v,down}-S_{ce,down}$ and $S_{ae,up}=S_{v,up}-S_{ce,up}$. The average vertical displacement during the effective aerial phase was calculated as $S_{ae}=(S_{ae,down}+S_{ae,up})/2$ (Fig. 4).

The total vertical displacement of the centre of mass at each step (Fig. 4) was calculated as the average between the total vertical displacement during the lift and that during the fall, i.e. $S_v=(S_{v,up}+S_{v,down})/2$.

The forward displacements of the centre of mass during t_{ce} and t_{ae} were labeled L_{ce} and L_{ae} (Fig. 4) and were calculated from the time integral of the instantaneous forward velocity of the centre of mass $V_f(t)$ during the corresponding times. These measures are more precise than those hitherto made using the average forward speed $\overline{V}_f$ (Cavagna et al., 1988) because they take into account the difference in forward speed between the lower and the upper part of the vertical oscillation.

Vertical stiffness

The vertical stiffness (k_{vert} in Fig. 5) was calculated from the effective contact time t_{ce} on the assumption that this time represents the half-period of oscillation of the elastic system: $k_{vert}=M_b(\pi/t_{ce})^2$, where M_b is the body mass of each subject. Correspondingly, the resonant frequency of the bouncing system was calculated as $f_s=1/(2t_{ce})$ (Fig. 5). The mass-specific vertical stiffness, k_{vert}/M_b, was also calculated from the slope of a graph obtained by plotting the vertical acceleration of the centre of mass a_v as a function of the simultaneous vertical displacement of the centre of mass S_v during the effective contact time (positive values of a_v), as described by Cavagna et al. (1988). This method, however, was found to be drastically affected by the oscillations of a_v after foot contact, particularly at high speeds and at 1.3 ***g***. In fact, the mass-specific vertical stiffness, calculated in some of the records from the maximum compression of the spring as $a_{v,mx}/S_{ce}$ (see Discussion) approaches that calculated from the effective contact time t_{ce} and is higher, particular in the presence of large oscillations, than that measured from the average slope of the a_v–S_v plot.

Table 1. *Speeds at which the pairs of the listed variables are statistically different at each gravity level*

Speed	t_{ce} *vs* t_{ae}				S_{ce} *vs* S_{ae}				L_{ce} *vs* L_{ae}				*f vs* f_s			
	1 ***g***		1.3 ***g***		1 ***g***		1.3 ***g***		1 ***g***		1.3 ***g***		1 ***g***		1.3 ***g***	
(km h^{-1})	*F*	*P*	*F*	*P*	*F*	*P*	*F*	*P*	*F*	*P*	*F*	*P*	*F*	*P*	*F*	*P*
5	13.19	0.0004	11.14	0.0009	6.23	0.0133	ns		4.31	0.0390	ns		ns		ns	
6	7.33	0.0074	22.28	0.0001	4.20	0.0417	ns		ns		10.1	0.0016	ns		6.21	0.0132
7	ns		33.86	0.0001	4.43	0.0365	9.28	0.0025	ns		19.6	0.0001	ns		9.11	0.0028
8	ns		35.24	0.0001	ns		8.37	0.0041	ns		25.74	0.0001	ns		11.26	0.0009
9	ns		29.53	0.0001	ns		11.03	0.0010	ns		26.91	0.0001	ns		11.26	0.0009
10	ns		4.38	0.0372	ns		ns		ns		4.69	0.0310	ns		ns	
11	10.45	0.0014	11.39	0.0008	ns		6.95	0.0088	14.57	0.0002	15.46	0.0001	5.35	0.0217	ns	
12	11.41	0.0009	ns		ns		ns		18.77	0.0001	ns		6.73	0.0102	ns	
13	7.10	0.0083	ns		ns		ns		13.31	0.0003	ns		4.37	0.0378	ns	
14	21.35	0.0001	ns		ns		ns		45.84	0.0001	ns		13.73	0.0003	ns	
15	17.62	0.0001	ns		ns		ns		44.50	0.0001	ns		12.86	0.0004	ns	
16	7.74	0.0059	ns		ns		ns		22.06	0.0001	ns		5.99	0.0153	ns	

ns, not significant, i.e. $P \geq 0.05$.

Leg stiffness

McMahon and Cheng (1990) pointed out that the actual compression of the hypothetical spring over which the body bounces each step includes not only the lowering of the centre of mass after foot contact, but also the amplitude of the arc made by the extended spring in its rotation during contact. These authors calculated leg stiffness as the ratio between maximal vertical force attained during contact and length change of the leg taking place during the contact time t_c. This leg change extends beyond the amplitude of the oscillation of the spring–mass system and includes the beginning and the end of 'spring' loading, when the load–extension curve is often not linear. In this study, leg stiffness k_{leg} is calculated within the amplitude of the oscillation, i.e. during the effective contact time t_{ce}, as the ratio between the increment of the vertical force above body weight ($M_b a_{v,max}$) and the total length change of the hypothetical leg-spring during this time ($S_{ce}+\Delta Y$). The amplitude of the arc made by the extended spring in its rotation during t_{ce} was calculated as $\Delta Y = l(1-\cos\theta)$, where $\theta = \arcsin(L_{ce}/2l)$ and l is the hip-ground distance of each subject (0.87–1.03 m).

Statistics

The data collected as a function of running speed were grouped into 1 km h^{-1} intervals as follows: 5 to <6 km h^{-1}, 6 to <7 km h^{-1},.., 19 to <20 km h^{-1} and 20–20.5 km h^{-1} at 1 ***g***; and 5 to <6 km h^{-1}, 6 to <7 km h^{-1},.., 17 to <18 and 19 to <20.5 km h^{-1} at 1.3 ***g*** (no data in the 18 to <19 km h^{-1} range at 1.3 ***g***). The data points in the figures represent the mean ± S.D. in each of the above speed intervals and the figures near the symbols in Fig. 4A,D give the number of items in the mean. Given the limitations imposed by the experimental conditions, a different number of subjects and of steps analyzed contributed to the mean values reported at each speed. Comparison between groups of data at each speed (Tables 1 and 2) was made using a two-factors analysis of variance (ANOVA) with contrast (SuperANOVA version 1.11). The contrast analysis was not made for the four highest speed groups (>16 km h^{-1}) because, both at 1 ***g*** and at 1.3 ***g***, the number of items was too small (see Fig. 4A,D). For clarity, in some of the figures lines are drawn through all of the data using Kaleidagraph 3.6.4 linear or weighted fits, as indicated in the legend of each figure. The only purpose of these lines is to be a guide for the eye; they do not describe the underlying physical mechanism.

Results

The results are given in two sections. The dynamics of the rebound of the body during the running step is described in the first section from (i) the displacement of the centre of mass taking place during the different phases of the step (total and effective aerial phase, total and effective ground contact phase), and (ii) the relationship between naturally selected step frequency and apparent resonant frequency of the bouncing system. The second section refers to the work done to lift and accelerate the centre of mass in a sagittal plane.

Dynamics of the rebound

In what follows an average is made of the upward and downward displacements, and corresponding time intervals, in the lower and upper half of the vertical oscillation of the centre of mass. This procedure was followed by Cavagna et al. (1988) and is the basis of the spring–mass model (Blickhan, 1989; McMahon and Cheng, 1990), which assumes that during the running step the landing and take-off conditions are the same.

The step period (τ, Fig. 4A,D), the vertical displacement of the centre of gravity during each step (S_v, Fig. 4B,E) and the step length (L, Fig. 4C,F) are given as a function of running speed ($\overline{V}_f$) at 1 ***g*** and 1.3 ***g***. As proposed by Cavagna et al. (1988), τ, S_v and L are divided into two parts, corresponding to the lower and upper parts of the vertical oscillation of the centre of mass: a lower part taking place when the vertical force is greater than

the body weight (t_{ce}, S_{ce} and L_{ce}; Fig. 4, red squares), and an upper part taking place when the vertical force is smaller than body weight (t_{ae}, S_{ae} and L_{ae}; Fig. 4, blue triangles). For comparison, τ, S_v and L have also been divided, according to tradition, into parts occurring during the ground contact phase and the aerial phase (Fig. 4, dotted lines).

It can be seen that t_{ae}=t_{ce}, and L_{ae}=L_{ce} in a range of lower speeds at 1 ***g*** (<10 km h^{-1}) and of higher speeds at 1.3 ***g*** (>11 km h^{-1}; see Table 1). As in previous studies (Schepens et al., 1998), this trend is not so clear for S_{ae} and S_{ce} due to the larger scatter of the data. In addition, τ, S_v and L are on average smaller at 1.3 ***g*** than at 1 ***g***, mainly due to their reduction in the phase of the step where the vertical force is less than body weight, i.e. t_{ae}, S_{ae} and L_{ae} are on average smaller than t_{ce}, S_{ce} and L_{ce} at 1.3 ***g*** (Table 2).

The whole body vertical stiffness k_{vert}, the leg stiffness k_{leg}, the natural frequency of the bouncing system f_s and the freely chosen step frequency f are given in Fig. 5 as a function of running speed. Fig. 5A,C show the vertical stiffness and the leg stiffness. The vertical stiffness increases linearly with speed whereas the leg stiffness is about constant independent of speed. This is in agreement with the spring–mass model predictions and experimental results reported in the literature (McMahon and Cheng, 1990; Farley et al, 1993). It can be seen that gravity tends to increase stiffness, but its effect is not significant at intermediate running speeds (Fig. 5C and Table 2).

In Fig. 5B,D a comparison is made between the step frequency f and the natural frequency of the bouncing system, f_s. At 1 ***g*** the overlap between f and f_s occurs at speeds (<11 km h^{-1}) lower than the speeds (>10 km h^{-1}) where the overlap occurs at 1.3 ***g*** (Table 1). As reported in previous studies (Cavagna et al., 1988; Schepens et al., 1998), the natural frequency of the bouncing system exceeds the step frequency beyond 10 km h^{-1} at 1 ***g*** (f_s>f, see Fig. 5 and Table 1). The maximum speed where f=f_s is greater at 1.3 ***g***. Data in Figs 4, 5 and Table 1 also suggest an asymmetry in the opposite direction at low speeds (t_{ce}>t_{ae} and f>f_s), particularly at 1.3 ***g***; this will be discussed below.

If the frequency of the bouncing system is calculated from the total contact time as f_c=1/(2t_c) or from the leg stiffness as $f_{k,leg}$=(k_{leg}/M_b)$^{0.5}$/(2π) (Fig. 5B,D, continuous lines), a large discrepancy is found with f. This indicates that the vertical stiffness only is related to step frequency.

Work

The step-average positive external power to move the centre of mass of the body in the sagittal plane is plotted as a function of the running speed in Fig. 6A (1 ***g***) and Fig. 6C (1.3 ***g***). Fig. 6B,D give the corresponding positive work done per unit distance. The results obtained at 1 ***g*** (Fig. 6A,B) are in good agreement with those obtained previously (e.g. Cavagna et al., 1976; Schepens et al., 1998). The external power, $\dot{W}_{ext}$, seems to increase linearly with speed. Since the gravitational potential energy curve and the kinetic energy curve of forward motion are nearly in-phase during the running step, the external power is practically equal to the sum of the power output due to the

Table 2. *Effect of gravity at each running speed (1* ***g*** *vs 1.3* ***g****)*

Speed (km h^{-1})	t_{ce}		t_{ae}		S_{ce}		S_{ae}		L_{ce}		L_{ae}		f		f_s		k_{vert}		$W_{ext/step}$	
	F	P	F	P	F	P	F	P	F	P	F	P	F	P	F	P	F	P	F	P
5	35.02	0.0001	25.56	0.0001	32.66	0.0001	8.87	0.0032	15.06	0.0001	5.83	0.0165	41.72	0.0001	22.26	0.0001	9.87	0.0019		ns
6	13.74	0.0003	22.53	0.0001	18.63	0.0001	8.12	0.0047	8.50	0.0039	8.11	0.0048	25.81	0.0001	8.52	0.0038	6.99	0.0087		ns
7	16.49	0.0001	48.81	0.0001	28.76	0.0001	19.11	0.0001	14.77	0.0002	22.93	0.0001	48.43	0.0001	14.93	0.0001		ns		ns
8	12.44	0.0005	70.27	0.0001	33.53	0.0001	30.40	0.0001	14.41	0.0002	42.00	0.0001	62.00	0.0001	13.36	0.0003	4.42	0.0364		ns
9	9.52	0.0022	70.40	0.0001	18.59	0.0001	25.75	0.0001	13.77	0.0003	53.22	0.0001	60.91	0.0001	10.94	0.0011		ns		ns
10		ns	26.55	0.0001		ns		ns	5.17	0.0238	26.85	0.0001	18.78	0.0001		ns	4.13	0.0431	20.63	0.0001
11		ns	49.26	0.0001		ns	9.01	0.0029		ns	51.52	0.0001	26.03	0.0001		ns		ns	10.67	0.0012
12		ns	18.92	0.0001		ns		ns		ns	22.84	0.0001	10.36	0.0014		ns		ns	11.74	0.0007
13		ns	14.76	0.0001		ns		ns		ns	19.72	0.0001	11.67	0.0007		ns	7.24	0.0076	5.71	0.0176
14		ns	16.96	0.0001		ns		ns	4.13	0.0432	30.02	0.0001	15.92	0.0001		ns		ns	12.53	0.0005
15		ns	26.57	0.0001		ns	8.76	0.0034	5.39	0.0211	55.60	0.0001	26.17	0.0001		ns	15.31	0.0001		ns
16		ns	8.36	0.0042		ns		ns	7.89	0.0053	18.95	0.0001	14.75	0.0002	5.78	0.0169	8.23	0.0045		ns

ns, not significant, i.e. P≥0.05.

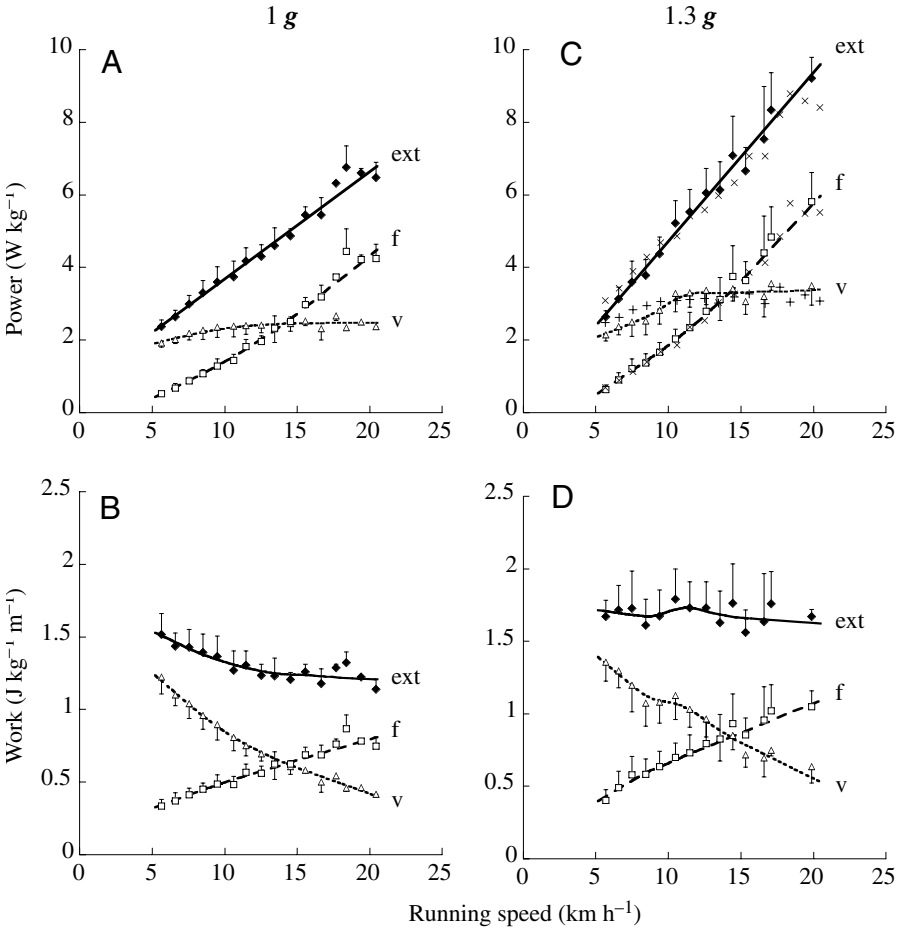

Fig. 6. External power and work per unit distance. (A,B) 1 ***g***, (C,D) 1.3 ***g***. The mass-specific power (A,C) and the mass-specific work done per unit distance (B,D) to maintain the movement of the centre of mass in the sagittal plane (filled diamonds, ext) to accelerate it forwards (open squares, f) and to lift it against gravity (open triangles, v) are given as a function of the running speed. In C, x and + give the mean values plotted in B ×1.3: the agreement with the experimental data shows that a 1.3× increase in gravity causes an ~1.3× increase in work. Lines for external power, $\dot{W}_{ext}$, are least-squares linear regressions of all the data, the other lines are weighted means of all the data (Kaleidagraph 3.6.4).

kinetic energy changes of forward motion $\dot{W}_f$ and the vertical lift against gravity $\dot{W}_v$, i.e. $\dot{W}_{ext} \approx \dot{W}_f + \dot{W}_v$. The power spent to sustain the forward velocity changes $\dot{W}_f$ increases with speed, whereas the power spent against gravity $\dot{W}_v$ attains a plateau at ~11 km h^{-1}. The external work done per unit distance, $\dot{W}_{xt}/\overline{V}_f$, is about constant at speeds greater than 10 km h^{-1}, due to mirror changes of $\dot{W}_f/\overline{V}_f$ and $\dot{W}_v/\overline{V}_f$, whereas it increases as the speed is reduced below 10 km h^{-1} due to the positive intercept of $\dot{W}_{ext}=f(\overline{V}_f)$ linear relation.

A 1.3× increase in gravity causes a ~1.3× increase of the external power $\dot{W}_{ext}$ and its components $\dot{W}_f$ and $\dot{W}_v$. This is shown by the similarity of the experimental data in Fig. 6C, with the crosses obtained by multiplying the mean experimental values of Fig. 6A (1 ***g***) ×1.3. The linear relationship between external power and speed is retained but power increases more steeply with speed from a smaller intercept at 1.3 ***g***. Given the small intercept, the slope approaches the work done per unit distance (Fig. 6D).

Discussion

Symmetric and asymmetric rebound

Running on Earth the step frequency is adapted to comply with the resonant frequency of the system (symmetric rebound) until a speed is attained (~11 km h^{-1}) where this is no longer possible (asymmetric rebound). The critical running speed is attained when the time-average vertical acceleration during the lower half of the oscillation, t_{ce}, which increases continuously with speed, exceeds the time-average acceleration during the upper half of the oscillation, t_{ae}, due to the pull by gravity. As hypothesized by Schepens et al. (1998) this limit is attained at a higher speed at higher gravity. A 30% increase in gravity increases the speed where the rebound can remain symmetric by ≈5 km h^{-1} (Fig. 5).

What is the physiological significance of attaining equivalent step frequencies and resonant bouncing frequencies? Runners maintain spring-like mechanics over a wide range of speeds independent of the symmetry of the rebound (Blickhan, 1989; McMahon and Cheng, 1990; Seyfarth et al., 2002; Farley and Gonzalez, 1996). Furthermore, a mismatch of the resonant and step frequencies does not appear to result in greater work required to maintain the motion of the center of gravity (Fig. 6). However, energy expenditure, rather than mechanical work, may be considered in this respect. It is possible that the energy expenditure required to maintain the oscillation will be smaller when the rebound is symmetric than when it is asymmetric. When the rebound is symmetric the system is activated to bounce at a frequency equal to its resonant frequency. The utility to adopt a step frequency equal to the resonant frequency of the bouncing system is suggested by the finding that at running speeds less than about 13 km h^{-1}, an increase in step frequency above the freely chosen step frequency increases the energy expenditure, despite a decrease in mechanical power (Cavagna et al., 1997).

At low running speeds the increase in gravity often causes an asymmetry in the opposite direction, with $t_{ce}>t_{ae}$ and $S_{ce}>S_{ae}$. This condition is also observed at 1 ***g*** in some subjects, particularly at low speeds, but is enhanced by an increase in gravity in all subjects (Fig. 4 and Table 1). The reversed asymmetry is due to the fact that the vertical stiffness when the vertical force is greater than body weight is, in some conditions, smaller than the vertical stiffness when the vertical force is less than body weight and the foot is still in contact

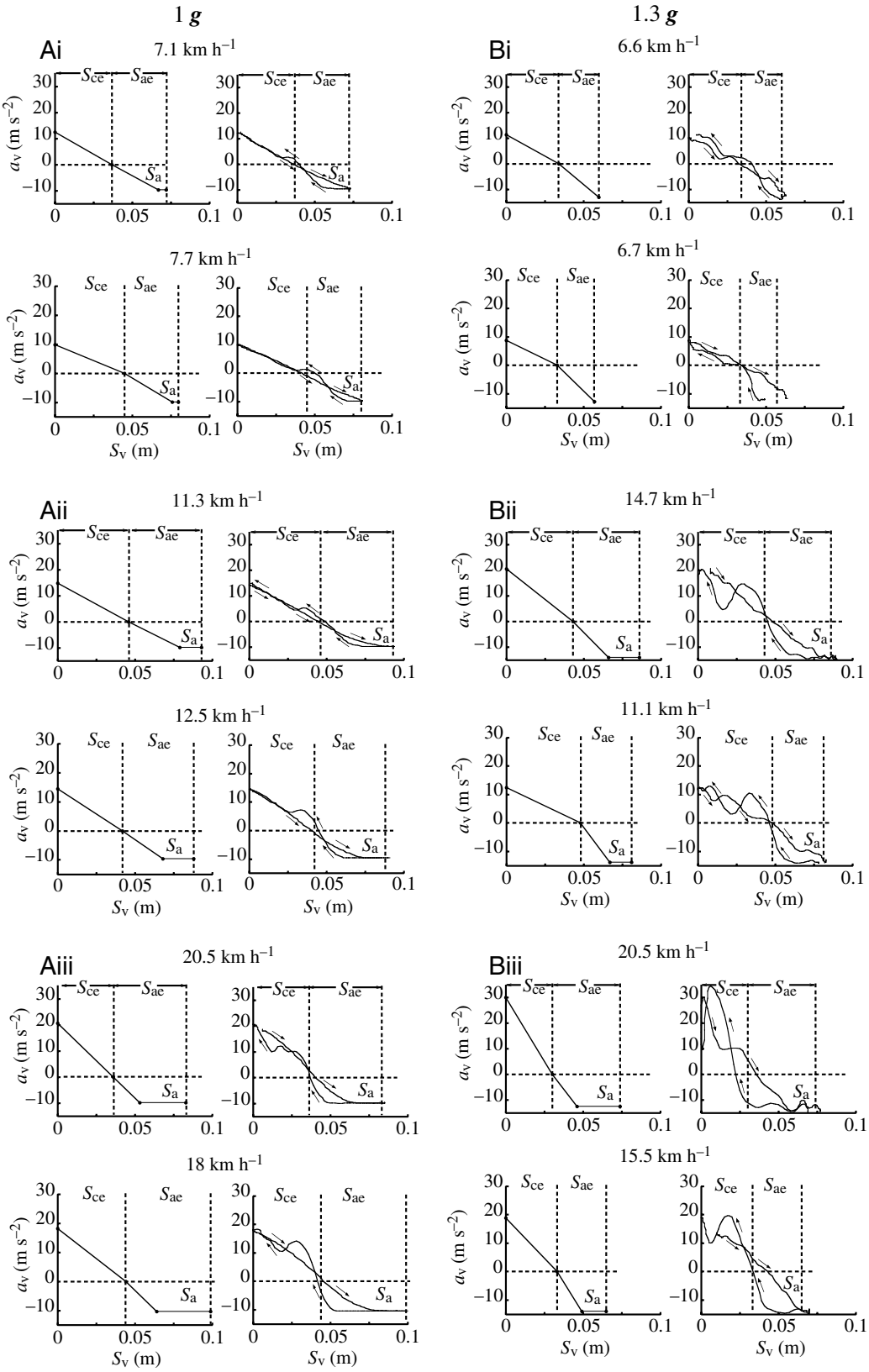

Fig. 7. Relationship between vertical acceleration and vertical displacement of the centre of mass. (A) 1 ***g***, (B) 1.3 ***g***. In each group the top set of speeds refers to subject A and the lower set to subject D. In each column graphs are arranged in couples, with speed increasing from top to bottom, as indicated. In each couple the graph on the right is the experimental record of vertical acceleration (a_v) *vs* vertical displacement (S_v) of the centre of mass during the step. These curves are disturbed by a large oscillation during the fall (McMahon et al., 1987), and are more consistent with the spring–mass model during the lift (arrows directed rightward and downward). Additional oscillations at 1.3 ***g*** are due to the vibrations of the aircraft: these are clearly visible in Fig. 2 in the force platform records, but not in the acceleration records due to the high damping of the accelerometers (see Materials and methods). The left graph of each couple is constructed using three points on the ordinate: $+a_{v,mx}$, a_v=0 and $-a_{v,mx}$, corresponding to bottom, half and top of the vertical oscillation, and the lift–fall average of the measured values of S_{ce}, S_{ae} and S_a on the abscissa. The zero on the abscissa corresponds to the bottom of S_v when the upward acceleration, on the ordinate, is at a maximum, $a_{v,mx}$ (measured as the a_v peak following the early peak due to rapid deceleration of the foot after contact; McMahon et al., 1987). The end of S_{ce} (the beginning of S_{ae}) corresponds to a_v=0 by definition, i.e. to $F_v=M_b\boldsymbol{g}$. The end of S_{ae} corresponds to F_v=0 and to $-a_{v,mx}$=1 ***g*** (Ai–iii) or 1.3 ***g*** (Bi–iii). The mass-specific vertical stiffness measured during the lower half of the oscillation, $k_{vert,ce}/M_b=+a_{v,mx}/S_{ce}$ (the slope of the line from $a_{v,mx}$ to a_v=0), is similar to $k_{vert}/M_b=(\pi/t_{ce})^2$ calculated on the assumption that t_{ce} represents one half oscillation of the bouncing system (Fig. 5). The mass-specific vertical stiffness measured during the upper half of the oscillation when the foot is in contact with the ground, $k_{vert,ae\text{-}a}/M_b=|-a_{v,mx}|/(S_{ae}-S_a)$ (the absolute value of the slope of the line from a_v=0 to $-a_{v,mx}$), differs, in some conditions, from the mass-specific vertical stiffness during the lower half of the oscillation, $k_{vert,ce}/M_b$. In particular, $k_{vert,ae-a}>k_{vert,ce}$ in some speeds at 1 ***g*** (subject D) and in a wider speed range at 1.3 ***g***: the significance of this finding is described in the text.

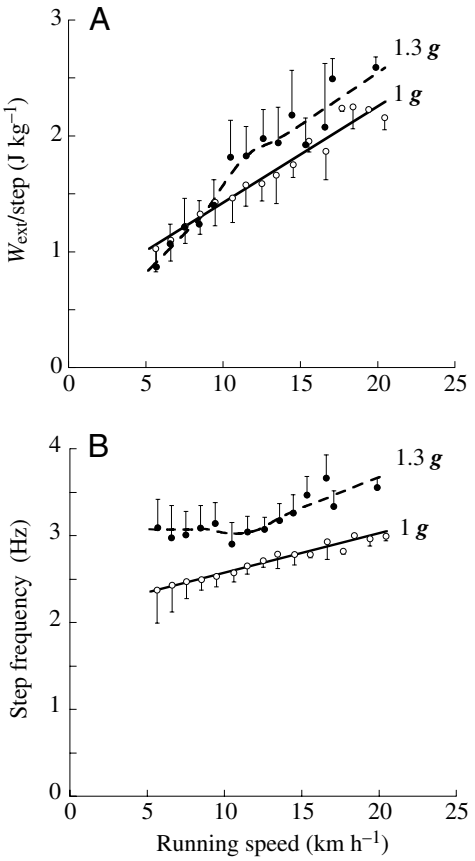

Fig. 8. The mass-specific external work done at each step (A) and the step frequency (B) are plotted as a function of running speed for the experiments made at 1 ***g*** (open circles) and at 1.3 ***g*** (filled circles). It can be seen that, on average, step frequency is increased by gravity more than the work per step: in other words, an increase in gravity increases the mechanical power output mainly through an increase in step frequency. Lines are least-squares linear regressions (1 ***g***) or weighted mean (1.3 ***g***) of all the data (Kaleidagraph 3.6.4).

with the ground. This is shown in Fig. 7, where the vertical acceleration of the centre of mass is plotted as a function of its vertical displacement for different running speeds.

The top row in each group (Ai, Aii, Aiii) Fig. 7A refers to subject A running at 1 ***g*** with a symmetric rebound, i.e. $S_{ce}{\approx}S_{ae}$, up to the speed of about 10 km h^{-1}: this is the average condition at 1 ***g*** (Cavagna et al., 1988; Schepens et al., 1998). The row below, however, refers to subject D running at a low running speed on Earth with $S_{ce}{>}S_{ae}$. It can be seen from Fig. 7A that in this case the mass-specific vertical stiffness measured during the lower half of the oscillation, $k_{vert,ae-a}/M_b{=}{+}a_{v,mx}/S_{ce}$ (the slope of the line from $a_{v,mx}$ to $a_v{=}0$), is lower than the mass-specific vertical stiffness measured during the upper half of the oscillation when the foot is in contact with the ground, $k_{vert,ce}/M_b{=}|{-}a_{v,mx}|/(S_{ae}{-}S_a)$ (the absolute value of the slope of the line from $a_v{=}0$ to $-a_{v,mx}$). As mentioned above, this condition is enhanced in both subjects by an increase in gravity to 1.3 ***g*** (Fig. 7B).

A vertical stiffness during S_{ae}–S_a, when the vertical force is lower than body weight, greater than that during S_{ce}, when the force is higher than body weight, does not reflect the characteristics of the elastic structures over which the body may possibly bounce. In fact, it has been shown both *in vitro* and *in situ* that the muscle–tendon stiffness increases with load (Hill, 1950; Cavagna, 1970; Ker et al., 1987). The finding that $k_{vert,ae-a}{>}k_{vert,ce}$ is simply due to the fact that body weight minus the upward push results in a restoring force, per unit of deformation of the spring, directed downward during t_{ae}–t_a, which is greater than that directed upward during t_{ce}. In these subjects, gravity during t_{ae} is more effective than the upward push of the elastic system during t_{ce} in absorbing and restoring the kinetic energy of vertical motion. Since the vertical momentum lost and gained during t_{ce} must equal the vertical momentum lost and gained during t_{ae}, a stiffer 'spring' during t_{ae}–t_a will contribute to make $t_{ae}{<}t_{ce}$ (Fig. 4) and, as a consequence, the step frequency, $f{=}1/(t_{ce}{+}t_{ae})$, greater than the natural frequency of the bouncing system, $f_s{=}1/(2t_{ce})$. This was in fact found during some of the runs at low speeds, particularly at 1.3 ***g*** (Fig. 5 and Table 1).

At low running speeds (<10 km h^{-1}), subjects characterized by $t_{ce}{\approx}t_{ae}$ and $S_{ce}{\approx}S_{ae}$ show a smaller angle swept by the leg during t_{ce}, a smaller S_v and a higher mass-specific vertical stiffness than subjects characterized by $t_{ce}{>}t_{ae}$ and $S_{ce}{>}S_{ae}$. Seyfarth et al. (2002) showed that different running strategies are compatible with stable running as predicted by a spring–mass system: 'either stiff legs with steep angles of attack or more compliant legs with flatter angles' (a steep angle of attack corresponds to a small angle swept by the leg during t_{ce}). The first strategy implies a smaller work done against gravity at each step, but a higher step frequency, with the result that the average vertical power is similar to that spent during the 'softer' running of the second strategy with $S_{ce}{>}S_{ae}$ (this was in fact measured comparing subject A with subject B, data not shown).

Effect of gravity on work

As shown in Fig. 6, a 1.3× increase in gravity results in an ~1.3× increase in the work done per unit distance against gravity and to sustain the forward speed changes. An increase in the work done against gravity is to be expected. The finding, however, that this increase is proportional to gravity gives the additional information that the average vertical displacement of the centre of mass per unit distance is the same at 1 ***g*** as at 1.3 ***g***. In other words, the sum of all the vertical lifts made in 1 km is the same and is independent of gravity. Since the step frequency is increased by gravity (Fig. 8 and Table 2), the vertical lift per step must be smaller at 1.3 ***g*** (Fig. 4), but the average lift per unit distance must be the same.

Less obvious is an increase with gravity of the work done per unit distance to sustain the forward speed changes. In fact kinetic energy of forward motion does not contain a gravity component. One possible explanation is given by a simplified model worked out by Alexander (*Modelling step by step*; http://plus.maths.org/issue13/features/walking/). Considering that the average vertical force over the step period (contact phase plus aerial phase) must equal body weight, Alexander derived an equation where the

work done per unit distance to sustain the forward speed changes of the centre of mass is proportional to gravity and to the tangent of the angle made by the leg with the vertical (leg is assumed as a rigid rod connecting point of contact on the ground with the centre of mass). Alexander's approach is based on the assumption that at each running step the direction of the resultant force exerted on the ground equals that of the link between centre of mass and point of contact on the ground. It follows that an increase in the vertical component of the force due to an increase in gravity, as in the present experiments, must imply an increase in the horizontal component as well. This is in agreement with the experimental results of Chang et al. (2000) showing that gravity affects both vertical and horizontal forces generated against the ground during running so that the orientation of the resultant vector remains aligned with the leg. This strategy, minimizing muscle forces, was first described by Biewener (1989). The finding that a 1.3× increase in gravity results in an ~1.3× increase in the work done to sustain the forward speed changes (Fig. 6) is in agreement with Alexander's equation, and indicates that at any given speed the average direction of the push is independent of gravity.

All together the above information suggest that, in running, a similar centre of mass motion tends to be maintained when gravity is increased as well as when stiffness of the ground is changed (Ferris and Farley, 1997; Ferris et al., 1998, 1999; Kerdok et al., 2002). The similarity here refers to the average vertical displacement per unit distance and the direction of the push, which are maintained in spite of an increase in step frequency.

The increase in external mechanical power induced by the increase in gravity is due to an increase in step frequency more than to an increase of the external work done at each step (Fig. 8, Table 2). The increase in step frequency in turn is explained to a lesser extent by an increase in the stiffness of the bouncing system (Fig. 5 and k_{vert} in Table 2), and to a greater extent by a decrease of the effective aerial time (Fig. 4 and t_{ae} in Table 2). He et al. (1991) found that the leg stiffness adopted at 1 ***g*** was retained when a lower gravity was simulated by suspension with springs.

The finding that the increase in step frequency $f=1/\tau=1/(t_{ce}+t_{ae})$, is not explained by an increase in the natural frequency of the bouncing system $f_s=1/(2t_{ce})$, but is mainly due to a shorter duration of the upper half of the oscillation t_{ae}, implies that the ratio t_{ce}/τ is greater at 1.3 ***g***. Since the average vertical force over the step period must equal body weight, a greater fraction t_{ce}/τ has the beneficial effect of reducing the fraction of the step during which the vertical force exerted on the ground is greater than body weight. On the other hand the greater step frequency at 1.3 ***g*** must increase the internal power spent to accelerate the limbs relative to the centre of mass (Cavagna et al., 1991).

List of symbols

$a_{v,mx}$ maximal vertical acceleration of the centre of mass of the body measured at the bottom ($a_{v,mx}$) and at the top ($-a_{v,mx}$) of the vertical displacement, S_v

E_{cm} translational energy of the centre of mass in the sagittal plane: $E_{cm}=E_k+E_p$

E_k translational kinetic energy of the centre of mass in the sagittal plane: $E_k=E_{kf}+E_{kv}$

E_{kf} kinetic energy of forward motion of the centre of mass: $E_{kf}=0.5M_bV_f^2$

E_{kv} kinetic energy of vertical motion of the centre of mass: $E_{kv}=0.5M_bV_v^2$

E_p gravitational potential energy of the centre of mass

f step frequency: $f=1/\tau$

f_c natural frequency of the bouncing system calculated from the total contact time: $f_c=1/(2t_c)$

$f_{k,leg}$ natural frequency of the bouncing system calculated from the leg stiffness: $f_{k,leg}=(k_{leg}/M_b)^{0.5}/(2\pi)$

f_s natural frequency of the bouncing system calculated from the effective contact time: $f_s=1/(2t_{ce})$

F_f fore–aft force exerted by the subject on the force platform

F_v vertical force exerted by the subject on the force platform

g acceleration of gravity

k_{leg} leg stiffness: $k_{leg}=(M_b a_{v,max})/(S_{ce}+\Delta Y)$, where $\Delta Y=l\{1-\cos[\arcsin(L_{ce}/2l)]\}$

k_{vert} vertical stiffness calculated from the effective contact time: $k_{vert}=M_b(\pi/t_{ce})^2$

$k_{vert,ae-a}$ vertical stiffness when the vertical force is less than body weight and foot is still in contact with the ground: $k_{vert,ae-a}=M_b|-a_{v,mx}|/(S_{ae}-S_a)$

$k_{vert,ce}$ vertical stiffness when the vertical force is greater than body weight: $k_{vert,ce}=M_b a_{v,mx}/S_{ce}$, this stiffness works out to be about equal to $k_{vert}=M_b(\pi/t_{ce})^2$

l hip–ground distance

L step length

L_a forward displacement of the centre of mass while the body is off the ground, calculated from the maximal forward speed attained during the step, $V_{f,mx}$, as: $L_a=t_aV_{f,mx}$

L_{ae} forward displacement of the centre of mass during t_{ae} calculated from the time integral of the instantaneous forward velocity of the centre of mass: $L_{ae}=\int_0^{tae}V_f(t)dt$

L_c forward displacement of the centre of mass while the body is on the ground: $L_c=L-L_a$

L_{ce} forward displacement of the centre of mass during t_{ce} calculated from the time integral of the instantaneous forward velocity of the centre of mass: $L_{ce}=\int_0^{tce}V_f(t)dt$

M_b body mass

S_a vertical displacement during the aerial time: $S_a=(S_{a,up}+S_{a,down})/2$

S_{ae} vertical displacement during the effective aerial time: $S_{ae}=(S_{ae,up}+S_{ae,down})/2$

$S_{ae,down}$ downward vertical displacement during the effective aerial time: $S_{ae,down}=S_{v,down}-S_{ce,down}$

$S_{ae,up}$ upward vertical displacement during the effective aerial time: $S_{ae,up}=S_{v,up}-S_{ce,up}$

S_c vertical displacement during contact with the ground: $S_c=(S_{c,down}+S_{c,up})/2$

S_{ce} vertical displacement during the effective contact time: $S_{ce}=(S_{ce,down}+S_{ce,up})/2$

$S_{ce,down}$ vertical displacement during the downward deceleration of the centre of mass

$S_{ce,up}$ vertical displacement during the upward acceleration of the centre of mass

S_v total vertical displacement of the centre of mass: $S_v=(S_{v,down}+S_{v,up})/2$.

$S_{v,down}$ vertical displacement during the fall of the centre of mass

$S_{v,up}$ vertical displacement during the lift of the centre of mass

t_a time interval during which the body is airborne

t_{ae} effective aerial time: time interval during which the vertical force is smaller than body weight

t_c time interval during which the body is in contact with the ground

t_{ce} effective contact time: time interval during which the vertical force is greater than body weight

$\overline{V}_f$ average running speed

V_f instantaneous velocity of the centre of mass in forward direction

V_v instantaneous velocity of the centre of mass in vertical direction

W_{ext} external work done at each step to sustain the changes in the translational mechanical energy of the centre of mass during its motion in a sagittal plane, $E_{cm}=E_p+E_{kf}+E_{kv}$

W_f positive work done at each step to sustain the changes in the translational kinetic energy of the centre of mass E_{kf} in forward direction

W_k positive work done at each step to sustain the changes in the translational kinetic energy of the centre of mass in the sagittal plane, $E_k=E_{kf}+E_{kv}$

W_v work done to sustain the changes in gravitational potential energy of the centre of mass E_p

$\dot{W}_{ext}$ step-average external power to move the centre of mass of the body in a sagittal plane: $\dot{W}_{ext}=\dot{W}_{ext}/\tau$

$\dot{W}_f$ step-average power to sustain the kinetic energy changes of forward motion: $\dot{W}_f=W_f/\tau$

$\dot{W}_v$ step-average power to sustain the vertical lift against gravity: $\dot{W}_v=W_v/\tau$

τ Step period, i.e. period of repeating change in the motion of the centre of mass

The authors would like to thank M. Roland and D. Theisen for their help in assembling and disassembling the apparatus on the aeroplane and G. Bastien, D. Harry, M. Legramandi and L. Tremolada for their help in the preparation of the LabVIEW software.

References

Alexander, R. McN. and Vernon, A. (1975). Mechanics of hopping by kangaroos (*Macropodidae). J. Zool. Lond.* **177**, 265-303.

Biewener, A. A. (1989). Scaling body support in mammals: limb posture and muscle mechanics. *Science* **245**, 45-48.

Biewener, A. A. (1998). Muscle-tendon stresses and elastic storage during locomotion in the horse. *Comp. Biochem. Physiol.* **120B**, 73-87.

Blickhan, R. (1989). The spring – mass model for running and hopping. *J. Biomech.* **22**, 1217-1227.

Cavagna, G. A. (1970). Elastic bounce of the body. *J. Appl. Physiol.* **29**, 279-282.

Cavagna, G. A. (1975). Force platforms as ergometers. *J. Appl. Physiol.* **39**, 174-179.

Cavagna, G. A., Saibene, F. P. and Margaria, R. (1963). External work in walking. *J. Appl. Physiol.* **18**, 1-9.

Cavagna, G. A., Saibene, F. P. and Margaria, R. (1964). Mechanical work in running. *J. Appl. Physiol.* **19**, 249-256.

Cavagna, G. A., Thys, H. and Zamboni, A. (1976). The sources of external work in level walking and running. *J. Physiol.* **262**, 639-657.

Cavagna, G. A., Franzetti, P., Heglund, N. C. and Willems, P. A. (1988). The determinants of the step frequency in running, trotting and hopping in man and other vertebrates. *J. Physiol.* **399**, 81-92.

Cavagna, G. A., Willems, P., Franzetti, P. and Detrembleur, C. (1991). The two power limits conditioning step frequency in human running. *J. Physiol.* **437**, 95-108.

Cavagna, G. A., Mantovani, M., Willems, P. A. and Musch, G. (1997). The resonant step frequency in human running. *Pflügers Arch.* **434**, 678-684.

Cavagna, G. A., Willems, P. A. and Heglund, N. C. (2000). The role of gravity in human walking: pendular energy exchange, external work and optimal speed. *J. Physiol.* **528**, 657-668.

Chang, Y.-H., Huang, H.-W., Hamerski, C. M. and Kram, R. (2000). The independent effects of gravity and inertia on running mechanics. *J. Exp. Biol.* **203**, 229-238.

Farley, C. T. and González, O. (1996). Leg stiffness and stride frequency in human running. *J. Biomech.* **29**, 181-186.

Farley, C. T., Glasheen, J. and McMahon, T. A. (1993). Running springs: speed and animal size. *J. Exp. Biol.* **185**, 71-86.

Ferris, D. P. and Farley, C. T. (1997). Interaction of leg stiffness and surface stiffness during human hopping. *J. Appl. Physiol.* **82**, 15-22.

Ferris, D. P., Louie, M. and Farley, C. T. (1998). Running in the real word: adjusting leg stiffness for different surfaces. *Proc. R. Soc. Lond. B* **265**, 989-994.

Ferris, D. P., Liang, K. and Farley, C. T. (1999). Runners adjust leg stiffness for their first step on new running surface. *J. Biomech.* **32**, 787-794.

He, J., Kram, R. and McMahon, T. A. (1991). Mechanics of running under simulated low gravity. *J. Appl. Physiol.* **23**, 65-78.

Heglund, N. C. (1981). A simple design for a force-plate to measure ground reaction forces. *J. Exp. Biol.* **93**, 333-338.

Hill, A. V. (1950). The series elastic component of muscle. *Proc. R. Soc. Lond. B* **137**, 273-280.

Ker, R. F., Bennett, M. B., Bibby, S. R., Kester, R. C. and Alexander, R. McN. (1987). The spring in the arch of the human foot. *Nature* **325**, 147-149.

Kerdok, A. E., Biewener, A. A., McMahon, T. A., Weyand, P. G. and Herr, H. M. (2002). Energetics and mechanics of human running on surfaces of different stiffnesses. *J. Appl. Physiol.* **92**, 469-478.

Margaria, R. (1938). Sulla fisiologia e specialmente sul consumo energetico della marcia e della corsa a varie velocità ed inclinazioni del terreno. *Atti Accad. nazionale Lincei Memorie* **7**, 299-368.

Margaria, R. and Cavagna, G. A. (1964). Human locomotion in subgravity. *Aerospace Med.* **35**, 1140-1146.

McMahon, T. A. and Cheng, G. C. (1990). The mechanics of running: how does stiffness couple with speed? *J. Biomech.* **23**, 65-78.

McMahon, T. A., Valiant, G. and Frederick, E. C. (1987). Groucho running. *J. Appl. Physiol.* **62**, 2326-2337.

Schepens, B., Willems, P. A. and Cavagna, G. A. (1998). The mechanics of running in children. *J. Physiol.* **509**, 927-940.

Seyfarth, A., Geyer, H., Günther, M. and Blickhan, R. (2002). A movement criterion for running. *J. Biomech.* **35**, 649-655.